Acoustic and Biomedical Engineering

Active Suspension Based on Low Dynamic Stiffness

J. Snamina*, J. Kowal and P. Orkisz
AGH — University of Science and Technology, Faculty of Mechanical Engineering and Robotics
Department of Process Control, al. A. Mickiewicza 30, 30-059 Krakow, Poland

The paper presents an active vibration control system based on low dynamic stiffness of suspension. Using a simple two degrees-of-freedom system a few basic concepts of lowering suspension dynamic stiffness are presented. Through reducing the dynamic component of force between the protected subsystem and remaining part of the system, considerable vibration suppression is achieved. Linear and nonlinear algorithms are proposed. In the case of nonlinear control algorithm, the sufficient link between the protected subsystem and the remaining part of the system necessary to change the position of the protected subsystem is maintained. Experiments described in the paper cover two different cases. In the first case, the suspension operated as the passive suspension, while in the second case, the active reduction system was included. The results are presented graphically.

DOI: 10.12693/APhysPolA.123.1118
PACS: 07.07.Tw, 46.40.–f, 05.45.–a

1. Introduction

In recent years there has been a significant growth in the design of suspension systems. This is associated with new solutions for innovative suspensions applied in vehicles, transport platforms, agricultural tractors, operator cabins and seats, etc. The effectiveness of suspensions depends on the control algorithms and the method of their implementation. Numerous methods used to tune the suspension parameters have been described in the literature [1–4].

A suspension system performs two main functions. The first is to give support to the structure at the accepted static deflection. In addition, suspension systems in cars have to ensure good contact between the wheels and the surface of the road. Thus the conventional suspensions are usually very stiff. The second function is associated with the vibroisolation of car bodies, operator seats, and platforms used to transport equipment sensitive to vibration. In this case, suspension should reduce vibration due to the external disturbances to the maximum possible degree. It is difficult to meet both requirements, since this involves opposing tendencies in the selection of the main parameters of suspension, i.e. stiffness and damping. Suspension should be rigid enough to effectively carry the static load, and soft enough to ensure the good isolation of vibrations. The design of suspension is always a compromise between handling and comfort.

Passive suspension systems can meet the basic requirements only to a limited degree. In designing effective suspension systems, only the active and semi-active systems offer great possibilities [5–7]. This explains their extensive development, both in terms of new theoretical concepts and practical solutions.

The present paper proposes the active methods for correction of the dynamic stiffness of suspension. The force generated by an active suspension subsystem changes the dynamic component of the force occurred in conventional suspension (which consists of spring and damper) leading to more effective isolation of the object being protected from vibration. Linear and non-linear control algorithms have been developed.

2. Mathematical model

Calculations were performed for a laboratory system shown in Fig. 1. The system consists of two masses that can move in vertical direction. The support of the system is connected with the moving part of the exciter.

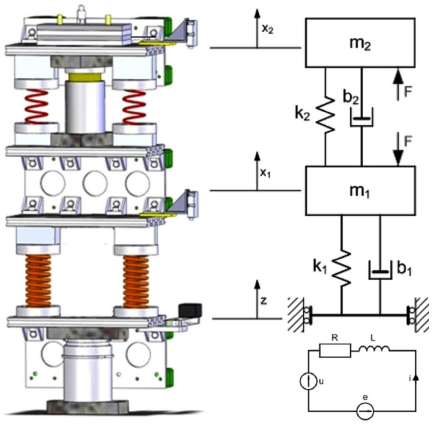

Fig. 1. Scheme of laboratory stand, mechanical and electrical subsystem.

The system proposed may be a simple model of many vibroisolated objects. For example, the same structure has a quarter-car model which is very commonly used for investigating the dynamics of a car suspension [1, 7]. Similarly, vibrations of sprung transport platforms can be, at the first approximation, studied with the proposed model.

In order to apply the control of vibrations in the suspension of the upper mass an actuator was introduced.

*corresponding author; e-mail: Snamina@agh.edu.pl

The role of the actuator was performed by a linear induction motor, placed in parallel with a spring and damper in the suspension of the upper mass.

It was assumed that the force exerted by the active subsystem does not depend on static component of coordinates and it is equal to zero at a static equilibrium position of the vibroisolated object. This assumption enables the separation of static and dynamic displacements in the systems. Equations describing the vibrations of both masses in relation to the static equilibrium position take the form

$$\begin{cases} m_1\ddot{x}_1 = k_1(z - x_1) + b_1(\dot{z} - \dot{x}_1) \\ \qquad -k_2(x_1 - x_2) - b_2(\dot{x}_1 - \dot{x}_2) - F(t) \\ m_2\ddot{x}_2 = k_2(x_1 - x_2) + b_2(\dot{x}_1 - \dot{x}_2) + F(t) \end{cases}, \quad (1)$$

where coordinates and coefficients are described in Fig. 1. The displacement $z(t)$ is realized by an exciter. $F(t)$ is the actuator force.

As shown in Fig. 1, the mechanical subsystem can be considered as a system with two inputs. The first input is associated with the displacement $z(t)$, the second with the force $F(t)$. Due to the fact that the linear induction motor was used as the actuator, the electrical subsystem should be described in the following considerations.

Fig. 1 shows the mechanical and electrical subsystems separately. In the calculations, the following simple equations were assumed to combine the electrical and mechanical subsystems:

$$\begin{cases} u = \kappa(\dot{x}_2 - \dot{x}_1) \\ F = \kappa i \end{cases}, \quad (2)$$

where κ is the motor constant. The equations above show that electrical power equals mechanical power.

The equation of the electrical subsystem resulting from the Kirchhoff's second law has the form

$$e = L\frac{\mathrm{d}i}{\mathrm{d}t} + Ri + u, \quad (3)$$

where L is the inductivity and R is the resistance of the linear motor winding.

Equations (1, 2) and (3) describe the state of the considered electromechanical system.

3. Linear control algorithms

The compromise between high stiffness of suspension needed to carry the load of the system and low stiffness due to the vibroisolation requirements can be achieved using an active system placed in vibroisolated objects suspension.

Supposing that the linear motor is supplied with a controlled source of voltage, it can generally be assumed that the supply voltage is a linear function of the state variables of the mechanical subsystem.

$$e = \alpha_{11}x_1 + \alpha_{12}\dot{x}_1 + \alpha_{21}x_2 + \alpha_{22}\dot{x}_2. \quad (4)$$

Using equations (2)–(4), the following differential equation describing the force generated by motor can be determined:

$$T\frac{\mathrm{d}F}{\mathrm{d}t} + F = \frac{\kappa}{R}(\alpha_{11}x_1 + \alpha_{12}\dot{x}_1 + \alpha_{21}x_2 + \alpha_{22}\dot{x}_2) - \frac{\kappa^2}{R}(\dot{x}_2 - \dot{x}_1). \quad (5)$$

In the equation, the time constant T of the motor circuit was introduced, which is the ratio of inductivity and resistance $T = L/R$. Equation (5) describes the feedback from the state variables of mechanical subsystem to its second input. For positive values of the coefficients, the feedback is positive and negative for the negative ones. The closed-loop system is shown in Fig. 2. Equations (1) and (5) describe the system after introduction the closed-loop control.

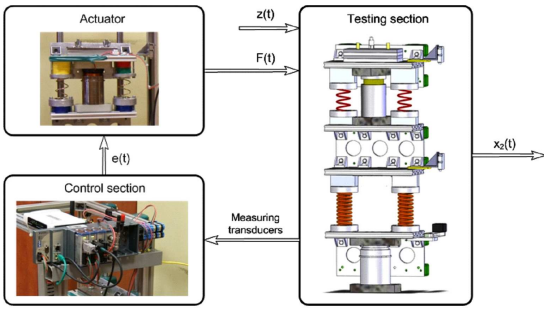

Fig. 2. Diagram of closed loop control system.

The character of the equation (5) indicates that for small time constants T, the first component on the left side of the equation will be small. Thus, the right side of the equation will describe the force generated by motor in an approximation form. To simplify further considerations and to make physical interpretation of results easier, it is convenient to write the equation describing the force F as follows:

$$T\frac{\mathrm{d}F}{\mathrm{d}t} + F = \beta_{11}k_2x_1 + \beta_{12}b_2\dot{x}_1 + \beta_{21}k_2x_2 + \beta_{22}b_2\dot{x}_2. \quad (6)$$

In equation (6), non-dimensional coefficients β_{11}, β_{12}, β_{21}, and β_{22} were introduced. The relationships between the proposed coefficients and those of the feedback introduced in the formula (5), are as follows:

$$\beta_{11} = \frac{\kappa}{Rk_2}\alpha_{11}, \quad \beta_{12} = \frac{\kappa}{Rb_2}\alpha_{12} + \frac{\kappa^2}{Rb_2},$$
$$\beta_{21} = \frac{\kappa}{Rk_2}\alpha_{21}, \quad \beta_{22} = \frac{\kappa}{Rb_2}\alpha_{22} - \frac{\kappa^2}{Rb_2}. \quad (7)$$

Using equations (1) and (6), the state equations of the closed system can be determined. They have the form

$$\begin{cases} \frac{\mathrm{d}x_1}{\mathrm{d}t} = v_1 \\ \frac{\mathrm{d}v_1}{\mathrm{d}t} = \frac{1}{m_1}\Big[-(k_1+k_2)x_1 - (b_1+b_2)v_1 \\ \qquad +k_2x_2 + b_2v_2 - F\Big] + \frac{1}{m_1}\Big[k_1z + b_1\dot{z}\Big] \\ \frac{\mathrm{d}x_2}{\mathrm{d}t} = v_2 \\ \frac{\mathrm{d}v_2}{\mathrm{d}t} = \frac{1}{m_2}\Big[k_2x_1 + b_2v_1 - k_2x_2 - b_2v_2 + F\Big] \\ \frac{\mathrm{d}F}{\mathrm{d}t} = \frac{1}{T}\Big[\beta_{11}k_2x_1 + \beta_{12}b_2v_1 + \beta_{21}k_2x_2 \\ \qquad +\beta_{22}b_2v_2 - F\Big] \end{cases}. \quad (8)$$

Analyzing the state equations, it can be easily noted that minimal vibration of the upper mass will occur when the

resultant dynamic force (the sum of spring force, damper force and the force generated by motor) is small. This condition is fulfilled when the non-dimensional coefficients take the following values: $\beta_{11} = -1$, $\beta_{12} = -1$, $\beta_{21} = 1$, $\beta_{22} = 1$. In this case the feedback can be described by the relative displacement of masses and the relative velocity. This is very convenient from the point of view of practical control because the relative displacement and relative velocity signals are available for measurement in all objects. When the time constant T of the motor approaches zero, the control leads to absence of resultant dynamic force between the lower and upper mass, and the motion of the upper mass becomes unstable and uncontrollable. If the time constant is greater than zero, the system is, of course, both stable and controllable.

In the other case of minimization of resultant dynamic force, the non-dimensional coefficients are $\beta_{11} = -1$, $\beta_{12} = -1$, $\beta_{21} = 0$, $\beta_{22} = 0$. To apply this control algorithm, it will be necessary to measure the displacement and velocity of the lower mass, which in practice can be difficult in some systems. When the time constant T of the motor approaches zero, the control leads to absence of influence of the lower mass on the movement of the upper mass, and its motion is no longer controllable but remains stable.

In the control algorithm of the dynamic stiffness proposed in this paper, it was assumed that the feedback depends only on relative displacement and relative velocity signals. The coefficients have to fulfil relationships $\beta_{21} = -\beta_{11}$, $\beta_{22} = -\beta_{12}$, and their modules have to be smaller than 1. Assuming $\beta_{21} = -\beta_{11} = \beta > 0$, and $\beta_{22} = -\beta_{12} = \beta > 0$, it can be shown that the control algorithm, as T approaches zero ($T \to 0$), is equivalent to the algorithm in which negative feedback from the upper mass acceleration $F = -\beta_a m_2 \ddot{x}_2$ was applied. The amplification coefficients fulfil the relationship $1+\beta_a = (1-\beta)^{-1}$. The algorithm based on negative feedback from the upper mass acceleration is also the control leading to the reduction of the dynamic stiffness of the upper mass suspension.

In each of algorithms described above, a component related to the negative feedback from the upper mass velocity can be added to the expression determining the motor reaction force, which as the time constant T approaches zero is the conventional skyhook control [8]. In this case, it is necessary to use a sensor for measuring the velocity signal $\dot{x}_2$.

To minimize the motor force in the ranges outside the resonances of the mechanical system, additional filters, decreasing the motor force in these ranges, can be added in the feedback loop. In such a case, outside the resonances, the active suspension operates in the same way as the passive suspension.

4. Nonlinear control algorithm

In algorithms proposed in the previous section, an actuator placed in the suspension of mechanical systems "weakens" the dynamic component of force between the protected subsystem and the remaining part of the system. However when the protected subsystem has to be moved as in the case of maneuvering vehicle or platform, the link between the protected subsystem and the remaining part of the system should be stiffened [9]. The relative displacement modulus between the protected subsystem and the remaining part of the system can be the criterion for making distinction between a signal associated only with vibration and a signal related to the necessity to change the position of the protected subsystem. It can be assumed that the signals associated only with vibrations are small, and those related with the movement of the system are larger. Such a criterion has many drawbacks but intuitively reflects the distinction between the two cases in question.

Description of the proposed control algorithm, including the assumed criterion, contains a non-dimensional, nonlinear factor in expression describing the voltage signal controlling the motor. The equation takes the following form

$$e = \alpha_0 (x_2 - x_1) \left(\left(\frac{x_2 - x_1}{\delta} \right)^2 + 1 \right)^{-4} + \alpha_{12} \dot{x}_1 + \alpha_{22} \dot{x}_2, \tag{9}$$

where parameter δ was introduced. It is apparent that the value of the proposed factor tends to one as $\frac{|x_2 - x_1|}{\delta}$ becomes small and to zero as $\frac{|x_2 - x_1|}{\delta}$ becomes large.

Utilizing equations (2, 3) and (9), the equation describing the force generated by linear motor takes the form

$$T \frac{\mathrm{d}F}{\mathrm{d}t} + F = \beta_0 k_2 (x_2 - x_1) \left(\left(\frac{x_2 - x_1}{\delta} \right)^2 + 1 \right)^{-4} + \beta_{12} b_2 \dot{x}_1 + \beta_{22} b_2 \dot{x}_2. \tag{10}$$

In the above formula, the following dimensionless coefficients were introduced which determine the multiplicity of the force components vs. the corresponding spring and damping forces in the upper mass suspension:

$$\beta_0 = \frac{\kappa}{R k_2} \alpha_0, \quad \beta_{12} = \frac{\kappa}{R b_2} \alpha_{12} + \frac{\kappa^2}{R b_2}, \quad \beta_{22} = \frac{\kappa}{R b_2} \alpha_{22} - \frac{\kappa^2}{R b_2}. \tag{11}$$

The state equations of the system with feedback can be presented as follows:

$$\begin{cases} \frac{\mathrm{d}x_1}{\mathrm{d}t} = v_1 \\ \frac{\mathrm{d}v_1}{\mathrm{d}t} = \frac{1}{m_1} \Big[-(k_1 + k_2) x_1 - (b_1 + b_2) v_1 + k_2 x_2 + b_2 v_2 - F \Big] + \frac{1}{m_1} \Big[k_1 z + b_1 \dot{z} \Big] \\ \frac{\mathrm{d}x_2}{\mathrm{d}t} = v_2 \\ \frac{\mathrm{d}v_2}{\mathrm{d}t} = \frac{1}{m_2} \Big[k_2 x_1 + b_2 v_1 - k_2 x_2 - b_2 v_2 + F \Big] \\ \frac{\mathrm{d}F}{\mathrm{d}t} = \frac{1}{T} \Big[\beta_0 k_2 (x_2 - x_1) \left(\left(\frac{x_2 - x_1}{\delta} \right)^2 + 1 \right)^{-4} + \beta_{12} b_2 v_1 + \beta_{22} b_2 v_2 - F \Big] \end{cases} . \tag{12}$$

On the basis of the above equations, simulations of the

motion of the system can be carried out. These equations are also very helpful in programming the control section of laboratory workstation.

5. The structure of the laboratory stand

In order to verify the proposed control algorithm an active vibration control system was designed. The laboratory stand was divided into three main parts: testing, measuring and control. The laboratory stand configuration is shown in Fig. 3.

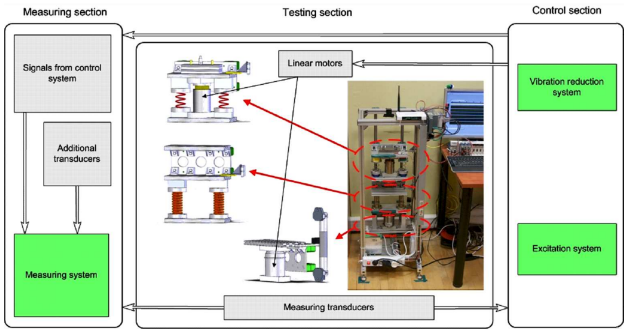

Fig. 3. Sections of the laboratory stand.

The testing section of the laboratory stand, shown also in Fig. 4, consists of a frame structure 1, to which the components of the vibration reduction system are mounted, as well as the converters and conditioning system parts. Three platforms 3, 7, 9 on linear bearings were designed between which the components of the tested vibration control system, such as the LA25 linear motor 5 and the spring sets 4, 8, are mounted. The first platform (support plate) is connected with moving part of the LA30 linear electro-dynamical motor 11 and the magnetostrictive displacement transmitter 10. The laboratory stand is additionally provided with incremental heads which are linear encoders 2, 6. The displacement transmitters were selected in order to achieve a high measuring resolution of 0.01 mm for platforms 3 and 7, and 0.1 mm for platform 9.

The complex structure of the control and measuring system made it necessary to divide it into two separate parts performing control and measurement functions, respectively. The measuring part comprises a CDAQ controller with three measuring cards. Each card allows for simultaneous recording of four analogue channels with a resolution of 16 bits at a maximum range of ± 10 V. The solution utilized allows the measuring channels to be recorded and scaled and the results to be saved on a PC connected to the measuring unit. The measuring converters used permit the recording of the displacement and acceleration of individual platforms and the current intensities in the linear actuator. The measuring system also enables recording taking into consideration the synchronization of the signals used in the control system such as the set value and regulation deviation values. The measuring system is provided with a graphic interface which facilitates the viewing of the current measuring

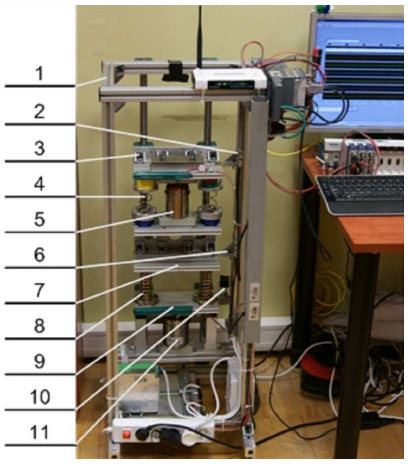

Fig. 4. Testing section of the laboratory stand.

signals being recorded and the selection of the location for files.

To build the control part a CRIO controller provided with a programmable array of logic gates FPGA was utilized [10]. It is composed of a real-time processor connected with the FPGA module via a data-bus. The module manages a data rail with a connection terminal for I/O cards. The TCP/IP communication modules allow the data imaging and operation of remote control panels to be controlled and measured, bearing in mind the simultaneous input of variables from multiple independent network locations such as a PC, for example, or an operator panel. Archiving the control data is made possible by means of exchanging data streams with Ethernet or sharing pre-saved files with the FTP service.

The tests were carried out using the LabView programming environment. The controller programming is a multi-staged process. The first stage defines the structure of the I/O modules; the data exchange is arranged by reserving appropriate memory blocks and data exchange channels assigned to them. The next stage is the preparation and compilation of the program to be executed by the FPGA module. The final stage involves preparation of a control program which will be executed by the real-time processor. Those tasks requiring a constant sampling period, as well as safety-related tasks, were performed in the FPGA system. Such a solution makes the system operation independent of the software, as the control algorithms are executed at the hardware level.

6. Laboratory tests of the active vibration control system

The laboratory stand allows for testing of active suspension in the ranges of frequency present usually in practice, up to 50 Hz. Experiment were done for the following parameters of the laboratory stand: $m_1 = 4.2$ kg, $m_2 = 3.9$ kg, $k_1 = 10500$ N/m, $k_2 = 6567$ N/m, $b_1 = 25$ Ns/m, $b_2 = 35$ Ns/m, similarly as in [11]. The support plate of laboratory stand was subjected to

transversal excitation $z(t)$. It was assumed sinusoidal excitation with growing frequency from 1 Hz to 15 Hz with constant angular acceleration 0.1 Hz/s. The angular acceleration was assumed as small that the system can achieved the almost steady-state motion for all frequencies from the range 1–15 Hz.

The displacements $x_1(t)$ and $x_2(t)$ as well as the excitation $z(t)$ were measured. Experiments were done in two cases. In the first case the active reduction system was excluded. Thus the suspension operated as the passive suspension. In the second case the active reduction system was included. In this case displacements $x_1(t)$, $x_2(t)$, and $z(t)$ are shown in Fig. 5.

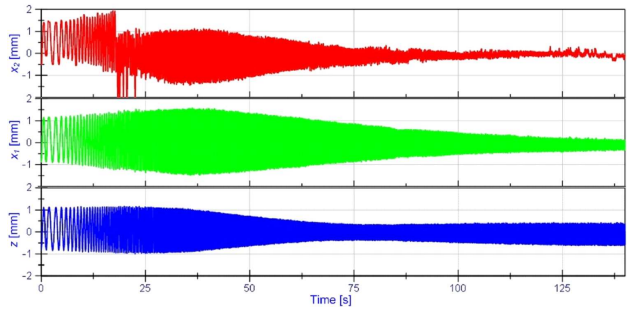

Fig. 5. Displacement time histories $x_1(t)$, $x_2(t)$, $z(t)$.

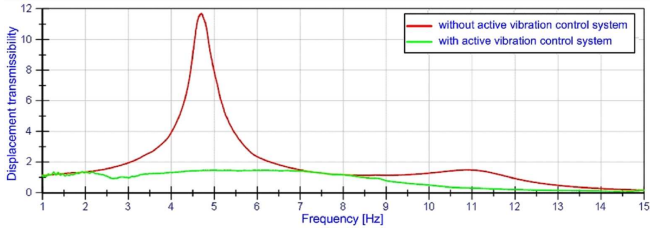

Fig. 6. Displacement transmissibility for the upper mass.

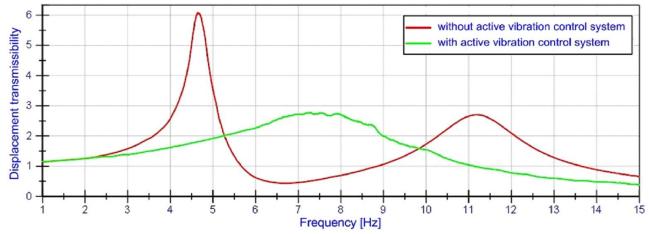

Fig. 7. Displacement transmissibility for the lower mass.

Using the registered displacements, the displacement transmissibilities were calculated in both cases. The comparisons of appropriate transmissibility curves for upper and lower mass of suspension are shown in Figs. 6 and 7.

For the considered system the modal analysis has been carried out. The first and second natural frequencies of the system without damping are $f_1 = 4.7$ Hz, $f_2 = 11.1$ Hz and corresponding modal vectors are as follows: $[1.0, 2.0]^T$, $[1.0, 0.5]^T$. The natural frequencies of the system with damping are equal to $f_1 = 4.7$ Hz, $f_2 = 11.0$ Hz. Elementary analysis of modal vector components shows that the displacement x_2 is dominant when the system vibrates in the first mode.

Displacement transmissibility curves for the system without vibration control have two peaks associated with natural frequencies. Operation of active vibration control system results in reduction of the value of displacement transmissibility for both the upper and the lower masses.

7. Summary

A few basic concepts aimed at lowering of suspension dynamic stiffness were presented using a simple two degrees of freedom system. Through reducing the dynamic component of force between the protected subsystem and remaining part of the system considerable vibration suppression was achieved. In the case of nonlinear control algorithm, the sufficient link between the protected subsystem and the remaining part of the system necessary to change the position of the protected subsystem was maintained. The laboratory stand allows comprehensive tests to be carried out on experimental vibration control systems.

Acknowledgments

This study is a part of the research project No. N N502213938.

References

[1] R. Rajamani, *Vehicle dynamics and control*, Springer, New York 2006.

[2] G. Genta, *Vibration of structures and machines*, Springer, New York 1999.

[3] A. Oustaloup, X. Moreau, M. Nouillant, *Control Eng. Practice* **4**, 1101 (1996).

[4] N. Yagiz, Y. Hacioglu, Y. Taskin, *IEEE Transactions on Industrial Electronics* **55**, 3883 (2008).

[5] M. Kolovsky, *Nonlinear dynamics of active and passive systems of vibration protection*, Springer, Berlin 1994.

[6] A. Alleyne, J.K. Hedrick, *IEEE Transactions on Control Systems Technology* **3**, 94 (1995).

[7] C.R. Fuller, S.J. Elliot, P.A. Nelson, *Active Control of Vibration*, Academic Press, London 1996.

[8] J. Snamina, A. Podsiadło, P. Orkisz, *Mechanics* **28**, 124 (2009).

[9] US Patent No. 7290642, *Magnetic spring device with negative stiffness* 2007.

[10] T. Topor-Kaminski, R. Żurkowski, M. Grygiel, *Acta Physica Polonica A* **120**, 748 (2011).

[11] P. Orkisz, *Mechanics and Control* **30**, 12 (2011).